

(NASA-TM-78606) AERODYNAMICS OF A  
TILT-NACELLE V/STOL PROPULSION SYSTEM (NASA)  
18 p HC A02/MF A01 CSCL 21E

N79-27138

Unclassified  
G3/07 27958

---

# Aerodynamics of a Tilt-Nacelle V/STOL Propulsion System

---

Mark D. Betzina and Michael D. Falarski

---

June 1979



National Aeronautics and  
Space Administration

AERODYNAMICS OF A TILT-NACELLE

V/STOL PROPULSION SYSTEM\*

Mark D. Betzina and Michael D. Falarski

Ames Research Center, NASA, Moffett Field, California

Abstract

Tests were performed in the Ames 40- by 80-Foot Wind Tunnel on a large-scale, tilt-nacelle V/STOL propulsion system to determine its aerodynamic characteristics. Results are presented in terms of unpowered nacelle aerodynamics and power-induced effects over an angle-of-attack range from 0 to 105°. It is shown that (1) the characteristics of the unpowered nacelle can be estimated with annular airfoil data, (2) the power-induced effects on the nacelle aerodynamics are significant, and (3) pitching moment can be correlated with lift and thrust.

\*Presented at Workshop of V/STOL Aerodynamics, Naval Postgraduate School, Monterey, California, May 1979.

### Introduction

A tilt-nacelle propulsion system, such as might be used on a V/STOL airplane, can be subjected to angles of attack greater than 90° during takeoff and landing maneuvers. These nacelles, which are large relative to the aircraft, have a significant effect on the aerodynamic characteristics of the aircraft. It is necessary, therefore, to be able to predict the aerodynamic characteristics of the nacelle so that the aerodynamics of the aircraft can be accurately represented.

Tests were performed in the Ames 40- by 80-Foot Wind Tunnel on a large-scale, tilt-nacelle V/STOL propulsion system, with the objective of determining its aerodynamic characteristics. Force and moment data were acquired from the wind tunnel balance system for various combinations of thrust and velocity at angles of attack from 0° to 105°. Results are separated into terms of unpowered nacelle aerodynamics and power-induced effects on nacelle aerodynamics. The unpowered nacelle characteristics are compared with those of an annular airfoil, the power-induced aerodynamics are discussed, and finally, in an attempt to establish a method for estimating the pitching moment produced by such a propulsion system, a relationship is determined between total lift and total pitching moment.

### Nomenclature

$A_F$	fan area, $1.206 \text{ m}^2 (12.98 \text{ ft}^2)$
$C_D$	wind axis drag coefficient, $\frac{D}{qA_F}$
$C_{D_{AERO}}$	aerodynamic drag coefficient, $C_D - C_{D_T}$
$C_{D_R}$	ram-drag coefficient, $\frac{D_R}{qA_F}$
$C_{D_T}$	drag coefficient due to thrust and ram drag, $C_{D_R} - C_J \cos \alpha$
$C_J$	thrust coefficient, $\frac{T}{qA_F}$
$C_L$	wind axis lift coefficient, $\frac{L}{qA_F}$
$C_{L_{AERO}}$	aerodynamic lift coefficient, $C_L - C_{L_T}$
$C_{L_T}$	lift coefficient due to thrust, $C_J \sin \alpha$
$C_m$	pitching-moment coefficient about the nacelle pivot axis, $\frac{M}{qA_F d}$
$d$	fan diameter, $1.397 \text{ m (4.583 ft)}$
$D$	total measured wind axis drag, N

ORIGINAL PAGE IS  
OF POOR QUALITY

ORIGINAL PAGE IS  
OF POOR QUALITY

$D_R$	ram drag, N
$L$	total measured wind axis lift, N
$M$	total measured pitching moment about the nacelle pivot axis, m - N
$q$	free-stream dynamic pressure, N/m <sup>2</sup>
$T$	total gross thrust, N
$\alpha$	nacelle angle of attack, deg

#### Propulsion System Description

Figure 1 shows the propulsion system in the Ames 40- by 80-Foot Wind Tunnel. The system consisted of a 1.4-m (55-in.), 13-bladed, variable-pitch fan driven by a Lycoming T55-L-11A, 2800 kW (3750 hp) gas turbine core engine. The fan was driven through a 4.75:1 gear reduction to a maximum speed of 3365 rpm; it had a bypass ratio of 17:1. Additional information on the fan and core engine is available in reference 1. The asymmetric inlet, designed for a tilt-nacelle lift/cruise fan propulsion system, had a higher contraction ratio on the windward side than on the leeward side; as a result, testing was possible at high angles of attack without stalling the fan. The cowling was designed to provide a nacelle suitable for wind-tunnel testing. The components of the propulsion system and its major dimensions are shown in figure 2. A more detailed description is available in reference 2. The nacelle was mounted about 4 m above the wind-tunnel floor on a single strut which was shielded from the wind by a fairing. The nacelle was rotated in a horizontal plane about the strut centerline for angle-of-attack variation.

#### Test Procedure and Data Reduction

Most of the data were acquired by varying thrust at constant nacelle angles of attack and at constant tunnel velocities. The operating limits of the propulsion system were determined and are discussed in reference 3. Tunnel velocity varied from 0-82 m/sec (0-160 knots) and angle of attack varied from 0°-120°. Thrust coefficients were computed from gross thrust, which was determined from total and static pressure and total temperature measurements in the inlet, fan duct, and core engine inlet. Gross thrust was varied up to a maximum of 30,700 N (6900 lb) by changing engine speed and fan blade angle. Ram drag was computed from inlet airflow, determined from static and total pressure measurements in the inlet, and from free-stream velocity. The unpowered-nacelle data were obtained with the fan blades feathered to minimize drag through the nacelle.

Force and moment data, obtained from the wind-tunnel balance system, were used to compute coefficients for the total nacelle forces and moments in the wind axis system. The fan area, 1.206 m<sup>2</sup>, and the fan diameter, 1.397 m, were used for the reference area and length, respectively. The moment center was located on the engine centerline, at the axis of rotation, 1.928 m aft of the inlet hilite.

## Results

### Basic Aerodynamics

Figure 3 shows the lift and drag characteristics of the propulsion system for thrust coefficient of 0, 10, and 20. The dashed lines represent the thrust and ram drag forces resolved into the lift and drag directions. Most of the resultant force on the nacelle is due to the thrust and ram drag forces; however, significant aerodynamic forces also are present, as shown by the difference between the solid and dashed lines in figure 3. At an angle of attack of 80° and a thrust coefficient of 10, 25% of the total lift is due to the nacelle aerodynamics.

### Induced Aerodynamics

In order to determine what part of the aerodynamic forces was induced by power, the aerodynamic lift and drag coefficients were plotted versus angle of attack (fig. 4). The coefficients were obtained by subtracting the thrust and ram drag components from the total lift and drag coefficients. There is a substantial difference between the powered and unpowered curves which represents the power-induced effect on the aerodynamic coefficients. The maximum aerodynamic lift in the powered case is about the same magnitude as the unpowered maximum lift, but it occurs at a much higher angle of attack. This indicates that, in the powered case, flow separation on the nacelle is delayed until the angle of attack is about 80°. The power-induced effect on the aerodynamic drag is very small at angles of attack less than 55°. The difference shown is probably due to the greater drag resulting from the fan blades and core engine in the unpowered case. At angles of attack greater than 55°, however, there is a large power-induced effect on the aerodynamic drag, which increases as power is increased. The maximum aerodynamic drag occurs at an angle of attack of 60° for the unpowered case, and at 75° to 90° for the powered case. Also shown in figure 4 are data for an annular airfoil with an aspect ratio of 1/3 (see ref. 4). The coefficients for the annular airfoil were converted to the same basis as those for the propulsion system, that is, inside area and diameter. Considering the difference in configurations, the annular airfoil portrays the nacelle quite accurately. The greater lift for the propulsion system may be due to the large fairing around the support strut, and the greater drag at low angles of attack may be a result of the fan blades and core engine. It is reasonable, therefore, to use annular airfoil data to estimate unpowered nacelle characteristics.

The aerodynamic lift to drag ratio is shown in figure 5. A comparison between the powered and unpowered data indicates a very small power-induced effect on this ratio. The data indicate a maximum lift-to-drag ratio of about 1.8, which occurs at an angle of attack of about 20°. Not enough data were acquired to define these curves at low angles of attack; however, it appears that there is a maximum lift-to-drag ratio at some low angle of attack that should be considered. The annular airfoil data, also shown in figure 5, are greater at low angles of attack because of the lower drag of the annular airfoil. The accuracy of the lift-to-drag ratio is questionable at low angles of attack, since the aerodynamic forces are small.

### Pitching-Moment Characteristics

The total pitching moment produced by the propulsion system is very large; it is shown as a function of angle of attack in figure 6. The maximum pitching moment occurs at angles of attack between  $75^\circ$  and  $90^\circ$  in the powered case, which is the same as the angle at which the maximum aerodynamic lift and drag occur. The total pitching moment consists of three parts: (1) aerodynamic pitching moment resulting from the aerodynamic forces on the nacelle, including power-induced effects; (2) moment produced by the flow turning into the inlet, which can be represented by the ram drag acting at an effective moment arm, and (3) moment caused by asymmetric fan thrust. Some asymmetry in the fan exhaust was present at high angles of attack, but the pitching moment resulting from it is a small percentage of the total and can be neglected. Therefore, the total pitching moment is primarily a result of both the ram drag and the nacelle aerodynamics. To assist in predicting pitching moments, it would be desirable to determine an effective ram drag moment arm. This requires separating the aerodynamic pitching moment from the pitching moment due to ram drag, however, because both contribute significantly. But this cannot be done quantitatively because the aerodynamic pitching moment is not known. Although the unpowered pitching moment, which agrees well with the annular airfoil data, is known, it does not include the power-induced effects. The power-induced effects on the aerodynamic forces were shown to be significant (fig. 4). But, since the location of these forces is unknown, their effect on pitching moment, although significant, cannot be determined. Therefore, the difference between the powered and unpowered data in figure 6 represents the sum of the ram-drag contribution and the power-induced effects on the nacelle aerodynamics.

In figure 7, the total nacelle pitching-moment coefficient is plotted versus the total lift coefficient. A good correlation between total lift and total pitching moment is indicated by the fact that for a given thrust coefficient, the data before and after maximum lift are near the same line. This correlation is shown in figure 8, where the ratio of total pitching-moment coefficient to total lift coefficient is shown as a function of thrust coefficient. This ratio changes only slightly with angle of attack at any given thrust coefficient. It is reasonable, therefore, to estimate the pitching moment of a tilt-nacelle V/STOL propulsion system for a given thrust coefficient as a percentage of the total lift, regardless of the angle of attack. Figure 8 indicates that this approximation results in a pitching-moment accuracy of about  $\pm 5\%$ .

### Conclusions

Although more testing is required to determine if the results presented in this paper are applicable to other configurations, the following conclusions can be made about a tilt-nacelle V/STOL propulsion system:

1. Unpowered-nacelle aerodynamics can be approximated by annular airfoil data for a similar aspect ratio.
2. Aerodynamic forces, including substantial power-induced effects, are a significant part of the total forces.

3. Very large pitching moments are produced and are a result of both ram drag and nacelle aerodynamics.

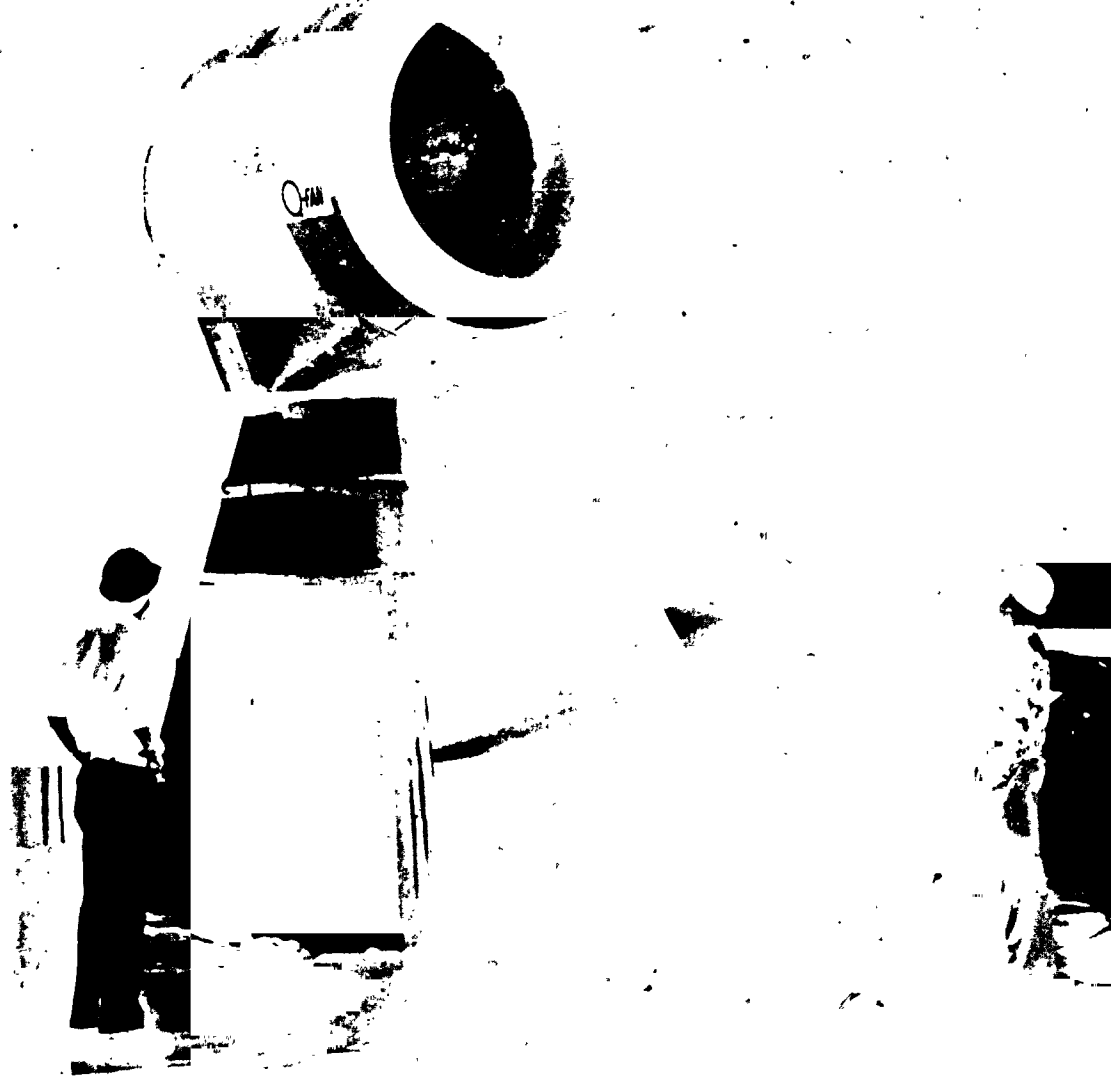
4. The maximum aerodynamic forces, as well as the maximum pitching moment, occur at angles of attack between 75° and 90°.

5. In order to determine an effective ram-drag moment arm, the aerodynamic pitching moment must be separated from the pitching moment due to ram drag.

6. Total pitching moment correlates well with total lift.

#### References

1. Demers, W. J.; Metzger, F. B.; Smith, L. W.; and Wainauski, H. S.: Testing of the Hamilton Standard Q-Fan Demonstrator (Lycoming T55-L-11A Core Engine). NASA CR-121265, March 1973.
2. Shain, W. M.: Test Data Report - Low Speed Wind Tunnel Tests of a Full Scale Lift/Cruise - Fan Inlet, With Engine at High Angles of Attack. NASA CR-152055, January 1978.
3. Syberg, J.: Low Speed Test of a High-Bypass-Ratio Propulsion System with an Asymmetric Inlet Designed for a Tilt-Nacelle V/STOL Airplane. NASA CR-152072, January 1978.
4. Fletcher, Herman S.: Experimental Investigation of Lift, Drag, and Pitching Moment of Five Annular Airfoils. NACA TN 4117, October 1957.



(a) 3/4 front view.

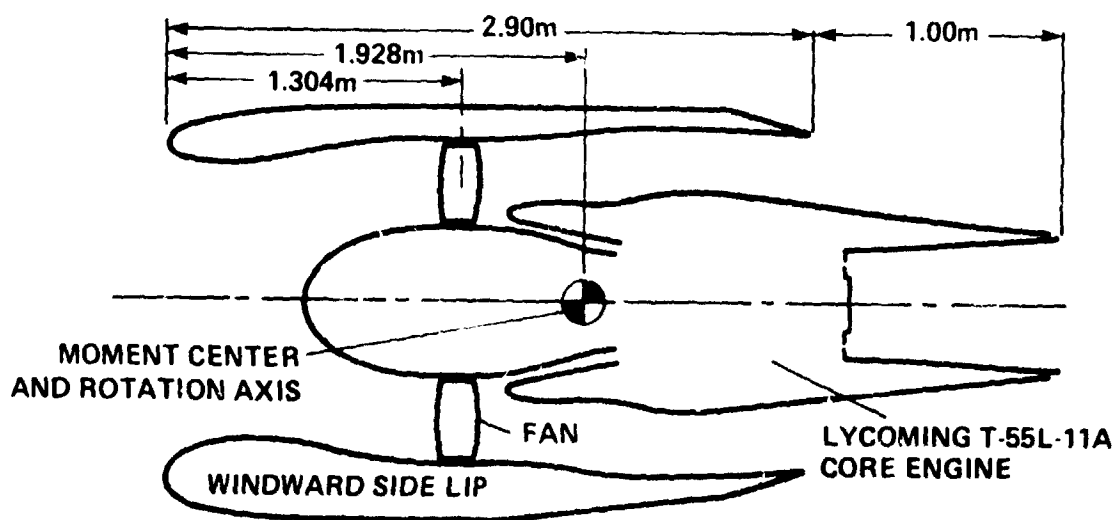
ORIGINAL PAGE IS  
OF POOR QUALITY

Figure 1.- Tilt-nacelle V/STOL propulsion system in the Ames 40- by 80-Foot Wind Tunnel.



(b) 3/4 rear view.

Figure 1.- Concluded.



BYPASS RATIO: 17:1  
MAX. FAN SPEED: 3365 rpm  
FAN AREA: 1.206m<sup>2</sup>  
FAN DIAMETER: 1.397m  
FAN EXIT AREA: 1.064m<sup>2</sup>  
CORE EXIT AREA: 0.25m<sup>2</sup>

Figure 2.- Nacelle schematic.

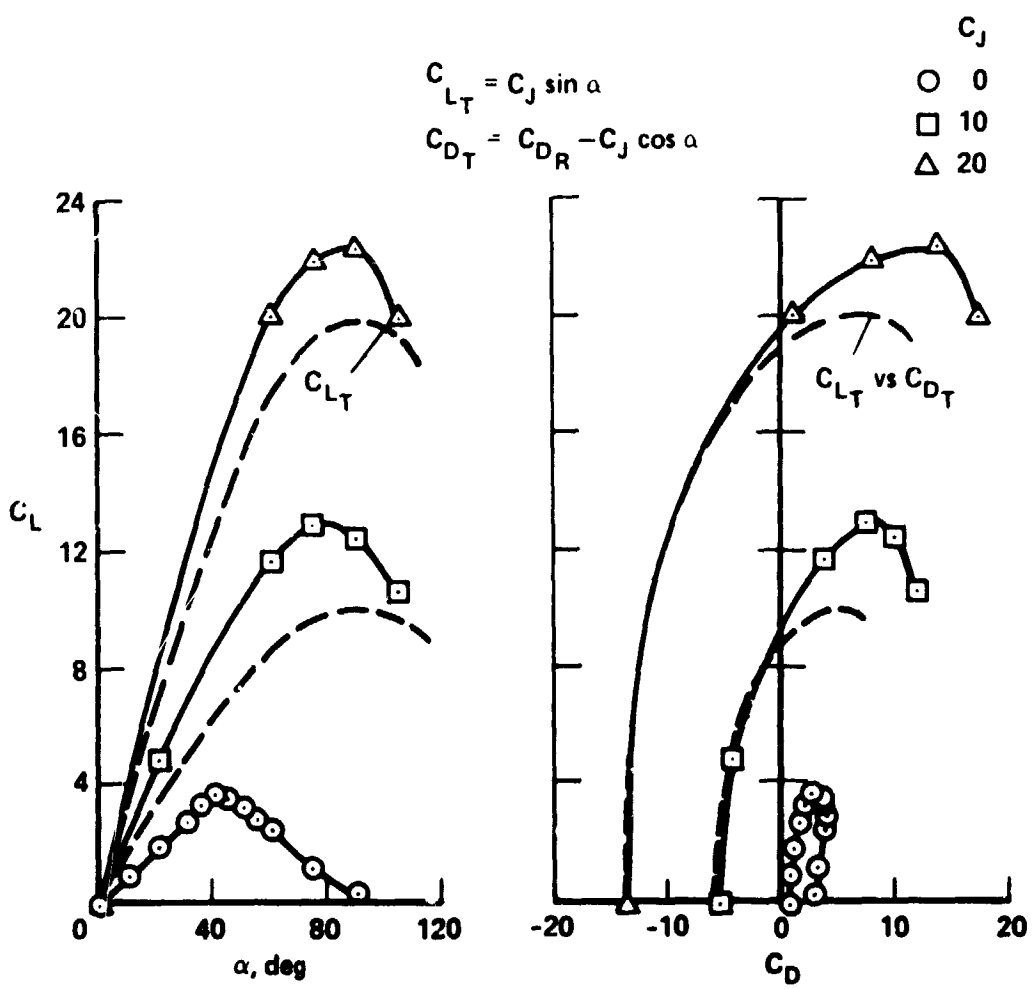


Figure 3.- Lift and drag characteristics.

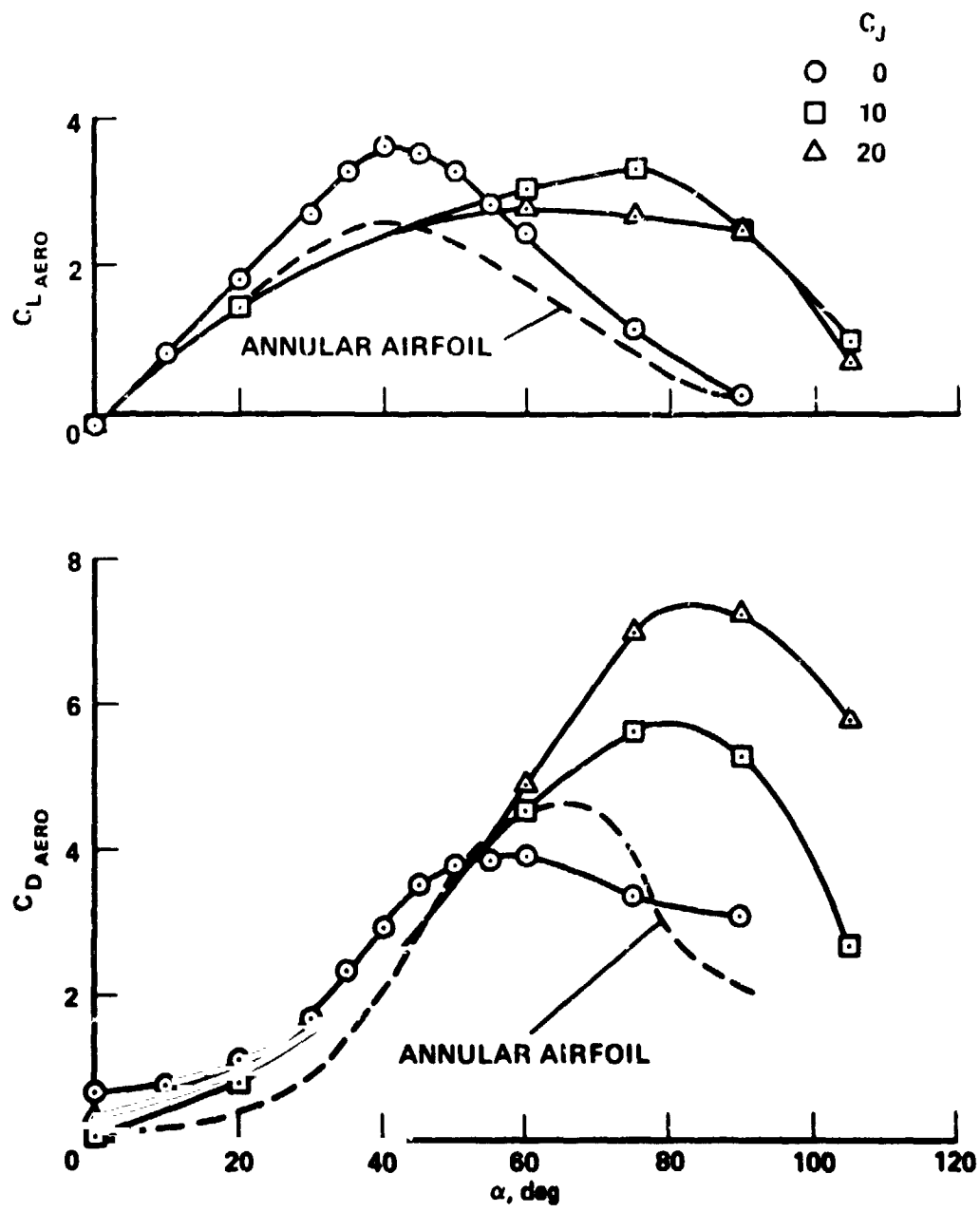


Figure 4.- Power-induced effect on aerodynamic lift and drag.

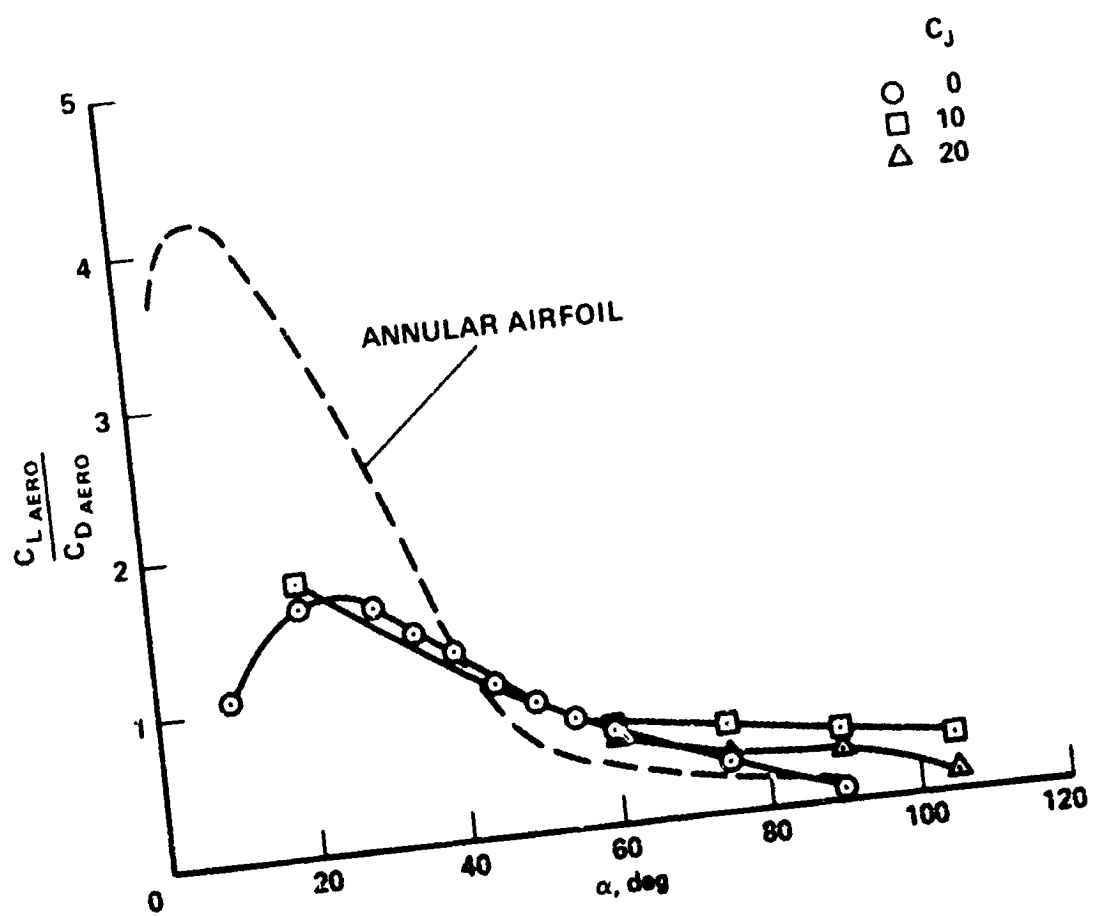


Figure 5.- Aerodynamic lift-to-drag ratio.

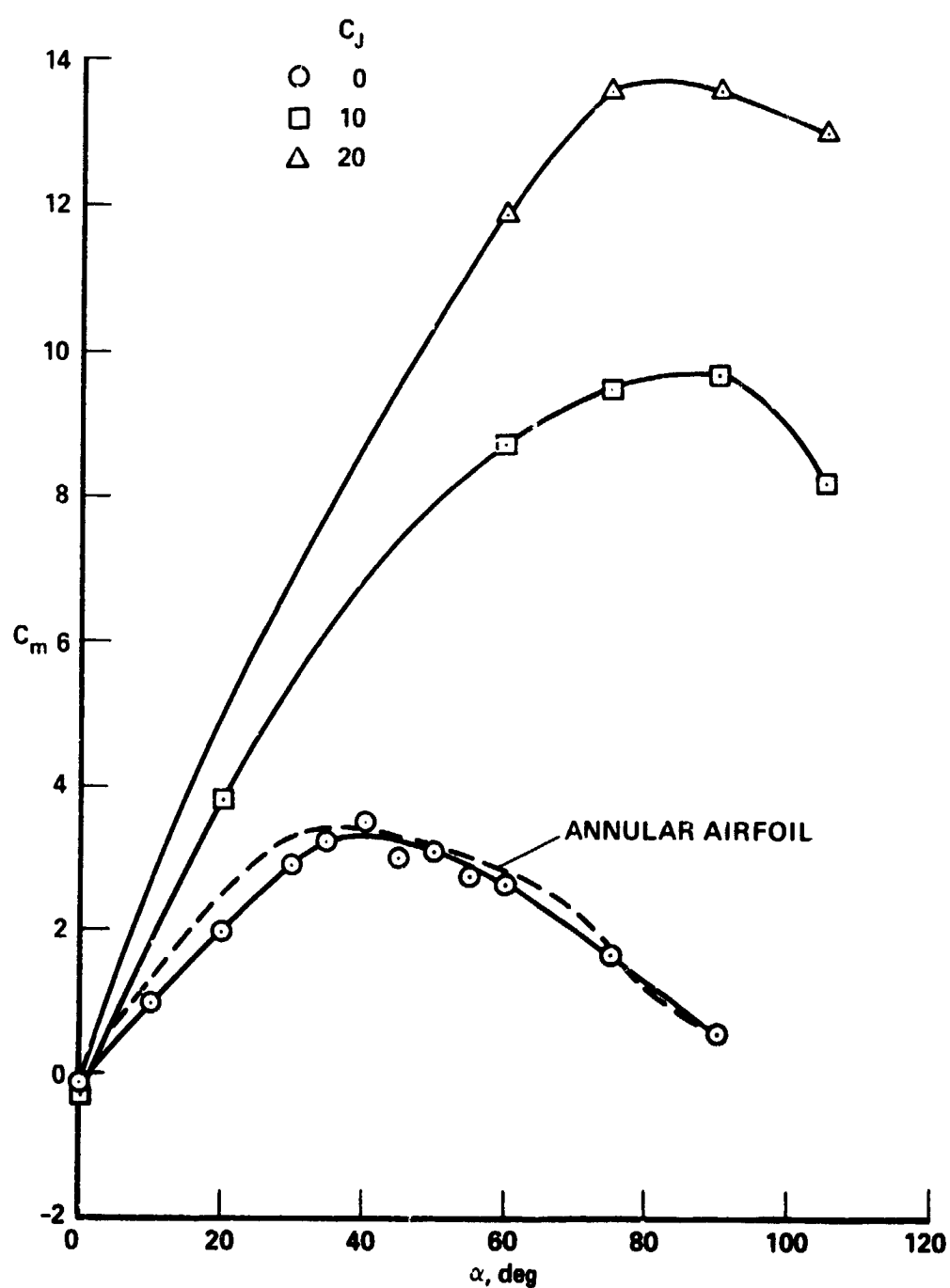


Figure 6.- Pitching moment vs angle of attack.

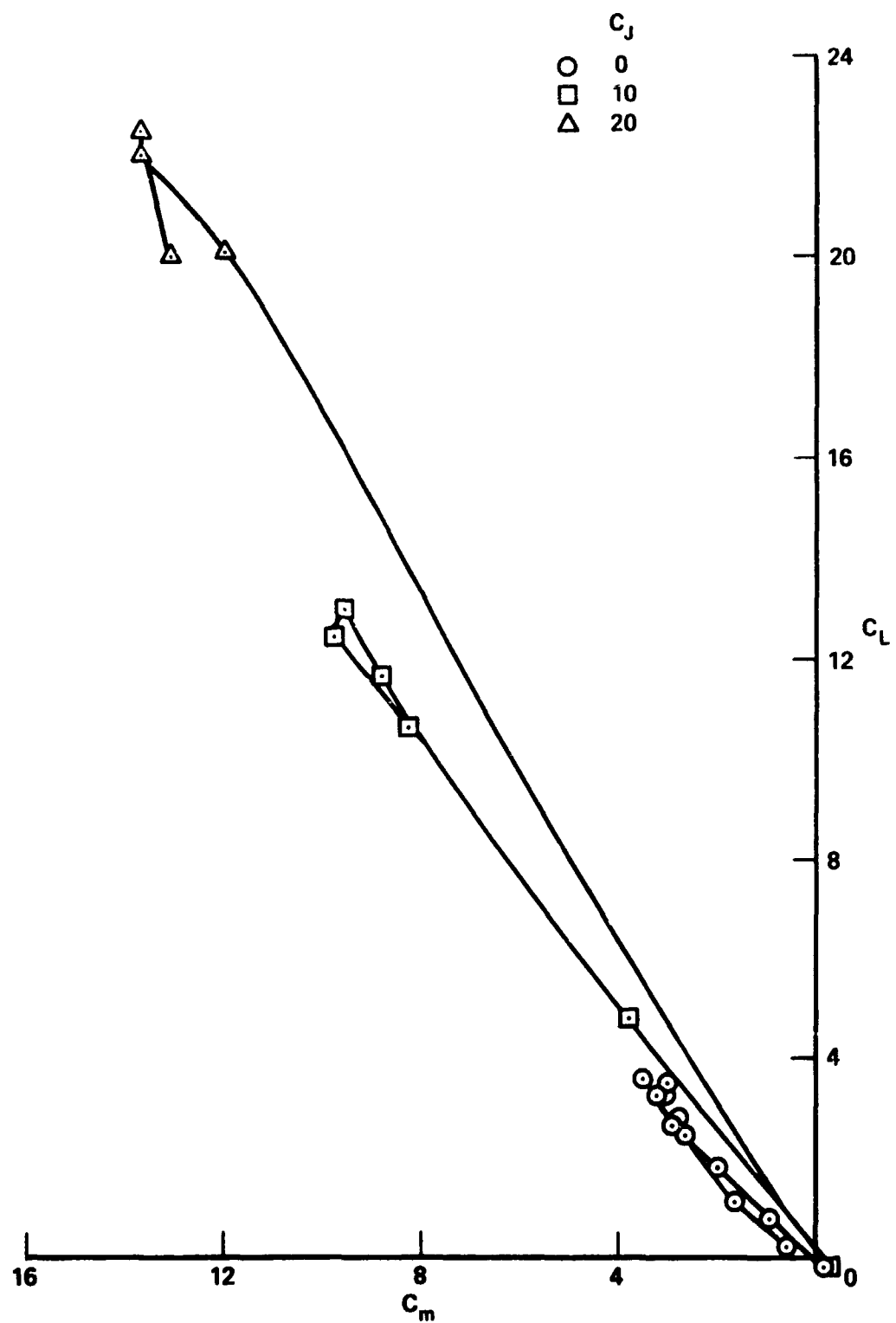


Figure 7.- Lift vs pitching moment.

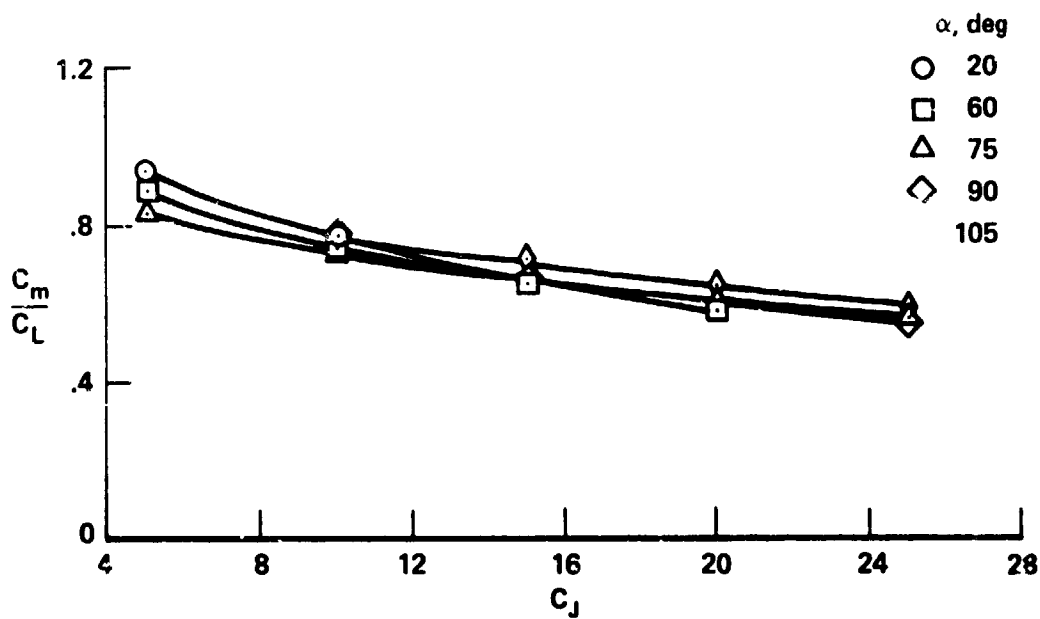


Figure 8.- Pitching moment to lift ratio.

1 Report No. NASA TM 78606	2. Government Accession No.	3 Recipient's Catalog No	
4 Title and Subtitle  AERODYNAMICS OF A TILT-NACELLE V/STOL PROPULSION SYSTEM*		5 Report Date	
		6. Performing Organization Code	
7 Author(s) Mark D. Betzina and Michael D. Falarski		8 Performing Organization Report No A-7849	
9 Performing Organization Name and Address  Ames Research Center, NASA Moffett Field, California 94035		10 Work Unit No 516-58-21	
12. Sponsoring Agency Name and Address  National Aeronautics and Space Administration Washington, D.C. 20546		11 Contract or Grant No	
		13 Type of Report and Period Covered Technical Memorandum	
		14 Sponsoring Agency Code	
15 Supplementary Notes  *Presented at Workshop of V/STOL Aerodynamics, Naval Postgraduate School, Monterey, California.			
16 Abstract  Tests were performed in the Ames 40- by 80-Foot Wind Tunnel on a large-scale, tilt-nacelle V/STOL propulsion system to determine its aerodynamic characteristics. Results are presented in terms of unpowered nacelle aerodynamics and power-induced effects over an angle-of-attack range from 0° to 105°. It is shown that (1) the characteristics of the unpowered nacelle can be estimated with annular airfoil data, (2) the power-induced effects on the nacelle aerodynamics are significant, and (3) pitching moment can be correlated with lift and thrust.			
17. Key Words (Suggested by Author(s))  V/STOL Tilt nacelle Aerodynamics Propulsion system		18. Distribution Statement  Unlimited  STAR Category 07	
19. Security Classif. (of this report) Unclassified	20. Security Classif. (of this page) Unclassified	21. No. of Pages 18	22. Price* \$3.50

\*For sale by the National Technical Information Service, Springfield, Virginia 22161